Cell and Tissue Research (2019) 375:641–654
https://doi.org/10.1007/s00441-018-2942-7

REGULAR ARTICLE

The effect of rho kinase inhibition on morphological and electrophysiological maturity in iPSC-derived neurons

Lise J. Harbom[1,2,3] · Taylor L. Rudisill[4] · Nadine Michel[2,3] · Karen A. Litwa[4] · Mark P. Beenhakker[1] · Michael J. McConnell[2]

Received: 7 May 2018 / Accepted: 5 October 2018 / Published online: 8 November 2018

Abstract

Induced pluripotent stem cell (iPSC)-derived neurons permit the study of neurogenesis and neurological disease in a human setting. However, the electrophysiological properties of iPSC-derived neurons are consistent with those observed in immature cortical neurons, including a high membrane resistance depolarized resting membrane potential and immature firing properties, limiting their use in modeling neuronal activity in adult cells. Based on the proven association between inhibiting rho kinase (ROCK) and increased neurite complexity, we seek to determine if short-term ROCK inhibition during the first 1–2 weeks of differentiation would increase morphological complexity and electrophysiological maturity after several weeks of differentiation. While inhibiting ROCK resulted in increased neurite formation after 24 h, this effect did not persist at 3 and 6 weeks of age. Additionally, there was no effect of ROCK inhibition on electrophysiological properties at 2–3, 6, or 12 weeks of age, despite an increase in evoked and spontaneous firing and a more hyperpolarized resting membrane potential over time. These results indicate that while there is a clear effect of time on electrophysiological maturity, ROCK inhibition did not accelerate maturity.

Keywords Rho kinase · Induced pluripotent stem cells · Excitability · Neuronal maturation · Y-27632

Introduction

Induced pluripotent stem cell (iPSC)-derived neuron technology provides a tractable model system to study the neurobiological consequences of genetic disorders in a human cell setting. Unlike embryonic stem cells, iPSCs allow the comparison of neurotypic control cells with those from a patient with a neurological disease. Since the first description of iPSCs (Takahashi et al. 2007), there has been great impetus to use the approach to model human neurological disorders including schizophrenia, autism and epilepsy (Bellin et al. 2012; Brennand et al. 2015).

Despite the identification of drug-sensitive, disease-relevant phenotypes, the electrophysiological behavior of iPSC-derived neurons appears immature relative to the neural activity observed in rodents or human-resected tissue (Bradford and McNutt 2015; Randall 2016). A depolarized resting membrane potential and high membrane resistance suggest that iPSC-derived neurons are comparable to neurons resected from human fetal tissue. Moreover, iPSC-derived neurons often produce low-amplitude, abortive action potentials that are similar to those frequently observed in the human fetal cerebral cortex (Livesey et al. 2016; Moore et al. 2009; Pre et al. 2014; Song et al. 2013). More thorough electrophysiological characterization has demonstrated that iPSC-derived neurons often develop, albeit slowly, more mature functional properties when cultured for months; nonetheless, these neurons remain immature relative to adult human

✉ Mark P. Beenhakker
markbeen@virginia.edu

✉ Michael J. McConnell
mikemc@virginia.edu

Lise J. Harbom
ljh4zu@virginia.edu

[1] Department of Pharmacology, University of Virginia School of Medicine, Charlottesville, VA 22903, USA

[2] Department of Biochemistry and Molecular Genetics and Neuroscience, Centers for Brain Immunology and Glia, Public Health Genomics, and Children's Health Research, University of Virginia School of Medicine, Charlottesville, VA 22903, USA

[3] Neuroscience Graduate Program, University of Virginia School of Medicine, Charlottesville, VA, USA

[4] Department of Anatomy and Cell Biology, Brody School of Medicine, East Carolina University, Greenville, NC 27834, USA

neurons (Belinsky et al. 2014; Chinchalongporn et al. 2015; Lam et al. 2017; Livesey et al. 2016; Moe et al. 2005; Nicholas et al. 2013; Pre et al. 2014; Weick 2016). Moreover, as long-term culturing procedures are labor-intensive and costly, there exists great interest to accelerate neuronal maturity.

Neuronal branching complexity is associated with more mature electrophysiological properties such as robust firing activity (Bardy et al. 2016). Neurite branching is in part regulated by the rho kinase pathway (Luo 2000). ROCK is a member of the Ras family of GTPases, which critically regulate cell adhesion and cytoskeletal rearrangement (Hall 1998). ROCK is activated by RhoA and phosphorylate myosin light leading to myosin activation and contraction of actin filaments, ultimately resulting in neurite retraction (Amano et al. 2000). In contrast, activation of the Rac1 pathway polymerizes actin, leading to neurite extension and synapse formation (Machesky and Hall 1997) (Fig. 1a).

ROCK inhibitors such as Y-27632 can be used to enhance the survival of embryonic stem cells and iPSCs by protecting against dissociation-induced apoptosis (Kurosawa 2012; Watanabe et al. 2007). ROCK inhibition enhances neurite outgrowth in multiple in vitro contexts, including cultured mouse neural stem cells (Gu et al. 2013; Jia et al. 2016), human NTERA-2 cells (Lingor et al. 2007; Roloff et al. 2015), human PC12 cells (Minase et al. 2010; Yang et al. 2010) and cultured dorsal root ganglion neurons from chicks and mice (Fournier et al. 2003; Yang et al. 2010). In vivo, ROCK inhibition promotes axonal outgrowth following CNS injury and contributes to injury recovery (Chan et al. 2005; Fournier et al. 2003; Lingor et al. 2007; Minase et al. 2010), leading to speculation that ROCK inhibition may have clinical potential in promoting nerve regeneration (Kubo et al. 2007; Tan et al. 2011).

While the effects of ROCK inhibition on neuron morphology are well-established, little information exists regarding how ROCK inhibition affects the electrophysiological properties of neurons. Given the correlation between morphological complexity and electrophysiological maturity seen in iPSC-derived neuron cultures, we sought to assess how ROCK inhibition during terminal differentiation of iPSC-derived neurons affects both morphological and electrophysiological properties. To this end, we plated iPSC-derived neurons in a 2D culture system and measured neurite branching, membrane properties and evoked a spontaneous firing activity of neuron cultures at different time points with and without Y-27632 treatment in early differentiation (Fig. 1b).

Materials and methods

Astrocyte culture Human cortical astrocytes were obtained from ScienCell (Carlsbad, CA, USA) and cultured in astrocyte media supplemented with astrocyte growth serum, FBS and pen/strep (ScienCell, Carlsbad, CA, USA). Astrocytes were passaged and split onto cell culture plates coated with 0.1% gelatin (Bio-Rad, Hercules, CA, USA). All neurons were cultured on coverslips on top of astrocyte-coated plates excluding the 24-h morphology experiments.

Generation of NPC lines iPSCs (line 9319 from Brennand et al. 2011) were maintained under standard conditions and dissociated from plates using collagenase type IV (Invitrogen, Carlsbad, CA, USA) to form floating embryoid bodies, which were cultured in DMEM/F12 + glutamax (Thermo Fisher Scientific, Waltham, MA, USA) supplemented with 1% N2 (Thermo Fisher Scientific, Waltham, MA, USA), 2% B27 without vitamin A (Thermo Fisher Scientific, Waltham, MA, USA), SB 431542 (Tocris, Bristol, UK) and LDN193189 (Stemgent, Cambridge, MA, USA). After 7 days, the embryoid bodies were re-plated onto polyornithine (Sigma-Aldrich, St. Louis, MP, USA) and laminin (Thermo Fisher Scientific, Waltham, MA, USA) coated plates and cultured in the same media for an additional 7 days until neural rosettes formed. Neural rosettes were dissociated using a neural rosette selection reagent (Stemcell, Vancouver, Canada) and replated onto Corning™ matrigel (Fisher Scientific, Hampton, NH, USA)-coated plates to form populations of neural progenitor cells (NPCs).

Neuron differentiation NPCs were grown until confluent and then plated at a density of 200,000 cells/well of a 6-well plate for 24-h neurite branching analysis; 100,000 cells per well of a 12-well plate for 3 and 6 week morphological analysis; and 50,000, 75,000, or 100,000 cells per well of a 12-well plate for electrophysiological analysis. For electrophysiological measurements, density did not have a significant effect on any measure (data not shown) so density groups were combined. For 24-h neurite analysis, NPCs were changed to neuron media (see below) for 24 h with Y-27632 (Selleck Chemicals, Houston, TX, USA) added as indicated, then fixed for immunohistochemistry. For 3- and 6-week morphological and all electrophysiological assays, NPCs were plated onto polyornithine/laminin-coated 18-mm coverslips and kept in NPC media for 48 h before being transferred onto astrocyte-coated plates in neuron media consisting of DMEM/F12 + glutamax supplemented with 1% N2 (Thermo Fisher Scientific, Waltham, MA, USA), 2% B27 (Thermo Fisher Scientific, Waltham, MA, USA), 20 ng/mL BDNF (Shenandoah Biotechnology, Warwick, PA, USA), 20 ng/mL GDNF (Shenandoah Biotechnology, Warwick, PA, USA), cyclic AMP (Sigma-Aldrich, St. Louis, MO, USA), ascorbic acid, pen/strep (Thermo Fisher Scientific, Waltham, MA, USA) and laminin (Thermo Fisher Scientific, Waltham, MA, USA) (morphology experiments only). Ten micrometers Y-27632 (Selleck Chemicals, Houston, TX, USA) was added for 1 to 2 weeks where indicated. Neurons were kept in culture for 3, 6, or 12 weeks as indicated. Media was changed every 5–7 days.

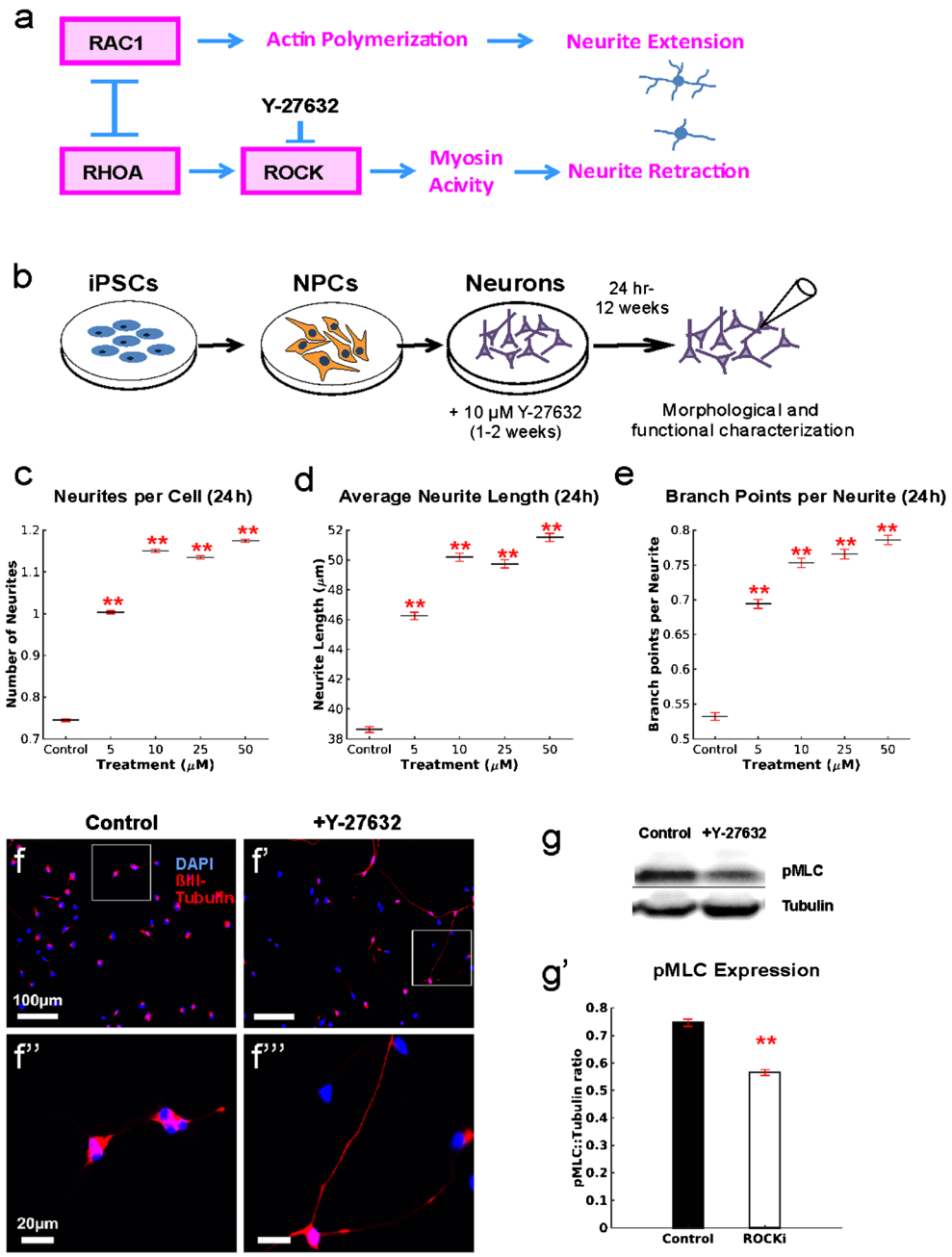

Fig. 1 Experimental setup and assessment of Y-27632 short-term effects. **a** The RAC1 and RHOA pathways regulate cytoskeletal rearrangement to cause neurite extension and retraction. ROCK is a substrate of RHOA and can be specifically blocked by the drug Y-27632. This decreases myosin phosphorylation leading to subsequent neurite retraction. **b** Neurotypic iPSCs are differentiated into a line of neural progenitor cells (NPCs). These are plated on coverslips and switched to neuron media (see methods). Neurons will be treated with or without Y-27632 in neuron media for the first 1–2 weeks after plating. **c**–**e** Neurons were treated with 0, 5,10, 25, or 50 μM Y-27632 for 24 h, stained with βIII-tubulin and DAPI and were automatically analyzed for neurite properties. The average number of neurites per cell (**c**, $p < 0.0001$; $n = 42{,}747$; 51,526; 56,953; 61,661; 57,269), average neurite length (**d**, $p < 0.0001$; $n =$ 22,022, 34,613, 41,918, 44,864, 57,269) and average number of branch points per neurite (**e**, $p < 0.0001$; $n = 22{,}022$, 34,613, 41,918, 44,864, 57,269) are significantly increased with all 4 tested concentrations compared to control cells. **f** Representative images of 24 h post-differentiation neurons treated with (**f'**, **f''**) or without (**f**, **f'')** 10 μM Y-27632, stained with neurite marker βIII-tubulin and DAPI. Bottom images (**f''**, **f'''**) are magnified views of insets shown in top images (**f**, **f'**). **g** Representative image (**g'**) and quantification (**g''**) of western blot of NPCs cultured with or without 10 μM Y-27632 for 24 h and probed for phosphorylated myosin regulatory light chain (pMLC) and tubulin as a loading control. Levels of pMLC relative to tubulin are decreased in Y-27632-treated cells ($n = 3{,}3$; $p < 0.0001$). Asterisk indicates $p < 0.05$. Double asterisks indicate $p < 0.001$ by 1-way ANOVA with post hoc HSD; data plotted as mean ± standard error of the mean (SEM); see Table 1 for complete statistics

Western blot NPCs were cultured for 24 h with or without 10 μM Y-27632 before being dissociated with Accutase (Innovative cell technologies, San Diego, CA, USA), pelleted and lysed in RIPA buffer consisting of 50 mM Tris HCl (pH 8.0), 150 mM NaCl, 1% NP-40, 0.5% sodium deoxycholate, 0.1% SDS, 10% NaF and 1 tablet of protease inhibitor (Sigma, 11836145001). Protein was quantified using the Pierce BCA assay kit (Thermo Fisher Scientific no. 23225) added to 2x Laemmli buffer (4% SDS, 10% 2-mercaptoethanol, 20% glycerol, 0.004% bromophenol blue, 0.125M Tris HCl, pH 6.8) and boiled for 10 min at 95°. For immunoblotting, 20 μg of total cell lysate was resolved by 4–15% Mini-PROTEAN precast gradient gel (Biorad no. 4561086). Proteins were transferred to a PVDF membrane for 90 min at 100 V and incubated at room temperature for 2 h in 3% BSA in TBS-T with antibodies anti-myosin pS19/pS20 (Rockland Immunochemicals, Pottstown, PA, USA; Cat no. 600-401-416) and anti-alpha tubulin (Thermo Scientific, Cat no. MS581P1). Blots were visualized with SuperSignal™ West Pico PLUS Chemiluminescent Substrate (Thermo Fisher Scientific, no. 34577) and a Bio-Rad ChemiDoc imaging system.

Twenty-four-hour neuron staining and morphological analysis After 24 h in neuron media containing 0, 5, 10, 25, or 50 μM Y-27632, cells were fixed with 4% formaldehyde with 4% sucrose. Cells were permeabilized for 2 min in 0.1% Triton X-100 (Sigma Aldrich, St. Louis, MO, USA) in PBS then incubated overnight at 4° with a primary antibody for βIII-tubulin (1 μg/mL, R&D systems, Minneapolis, MN, USA; Cat no. MAP 1195) in 2% goat serum-PBS, then incubated at room temperature for 1 h with a secondary antibody (4 μg/mL, Thermo Fisher Scientific, Waltham, MA, USA; Alexa Fluor goat anti-mouse 568) in 2% goat serum-PBS. Glass coverslips were mounted onto the wells using Vectashield Mounting medium with DAPI (Vector labs, Burlingame, CA, USA). Images were taken on a EVOS FL Auto 2 (Thermo Fisher Scientific, Waltham, MA, USA) at × 10 magnification and neurites were assessed using the CellInsight CX5 High Content Screening Platform (Thermo Fisher Scientific, Waltham, MA, USA) and quantified for the number, length and branching of neurites per cell (100 fields per well).

Three- and 6-week neuron staining and morphological analysis After 1 week of differentiation, neurons were transfected with an AAV inducing mCherry fluorophore expression driven by a synapsin promoter (AAV-hSyn-mCherry, Deisseroth in-stock AAV vectors, UNC vector core, Chapel Hill, NC, USA). At 3 and 6 weeks of age, cells were fixed in 4% PFA for 15 min and transferred into PBS until the time of staining. Cells were washed in 0.5% triton/PBS followed by permeabilization in 3% bovine serum albumin (BSA, Thermo Fisher Scientific, Waltham, MA, USA) in 0.1% triton in PBS (PBS-T) for 1 h at room temperature. Cells were left overnight at 4 °C in a primary antibody (1:1000, chicken anti-mCherry, Novus Biologicals Littleton, CO, USA; Cat no. NBP2-25158). The following day, cover slips were washed with PBS-T before applying a secondary antibody (1:1000, goat anti-chicken 555, Thermo Fisher Scientific, Waltham, MA, USA Alexa Fluor A-21437) for 1 h at room temperature. Cells were washed again with PBS-T and then incubated at room temperature in DAPI (1:1000, Thermo Fisher Scientific, Waltham, MA, USA) for 5 min before being transferred into water. Coverslips were mounted using prolong gold antifade mountant (Thermo Fisher Scientific, Waltham, MA, USA). Cells were then imaged at × 63 using the Neurolucida system (MBF Bioscience, Williston, VT) with an Axioskope microscope-driven stage and an AxioCam MRc camera (Zeiss Microscopy, Oberkochen, Germany). Neurites were manually traced and analyzed using Neurolucida and Neurolucida Explorer software.

Whole-cell patch clamping Neurons were recorded in artificial cerebrospinal fluid (ACSF) containing 0.25 mM potassium chloride, 1 mM glucose, 12.6 mM sodium chloride, 0.125 mM sodium phosphate, 0.1 mM magnesium sulfate, 0.2 mM calcium chloride and 2.6 mM sodium bicarbonate, adjusted with water to an osmolarity of ~ 300. Whole-cell patch clamping was performed with pipettes filled with potassium gluconate internal containing 100 mM potassium-gluconate, 9 mM magnesium chloride, 13 mM potassium chloride, 0.07 mM calcium chloride, 10 mM Hepes, 10 mM EGTA, 2 mM ATP and 0.5 GTP adjusted to an osmolarity of ~ 285.

Resting membrane potential was assessed by recording a 50-s long trial in current clamp with no applied current and averaging the measured membrane potential. Results shown are adjusted for liquid junction potential. Membrane resistance was assessed by voltage clamping the cell at − 70 mV and applying a 50 ms, 15 mV square pulse during each of 100 trials and then dividing the averaged resultant steady-state current by the voltage step.

Evoked and spontaneous activity were recorded in current clamp with a holding current to maintain ~ − 65 mV resting membrane potential. The cell was run through a ten-trial protocol, in which every trial contained a 1 s, + 25 pA depolarizing pulse to evoke firing activity.

Electrophysiology analysis All electrophysiology recordings were performed and analyzed using pClamp™ and Clampfit™ software (Molecular Devices, LLC, San Jose, CA, USA). Action potentials were manually measured from

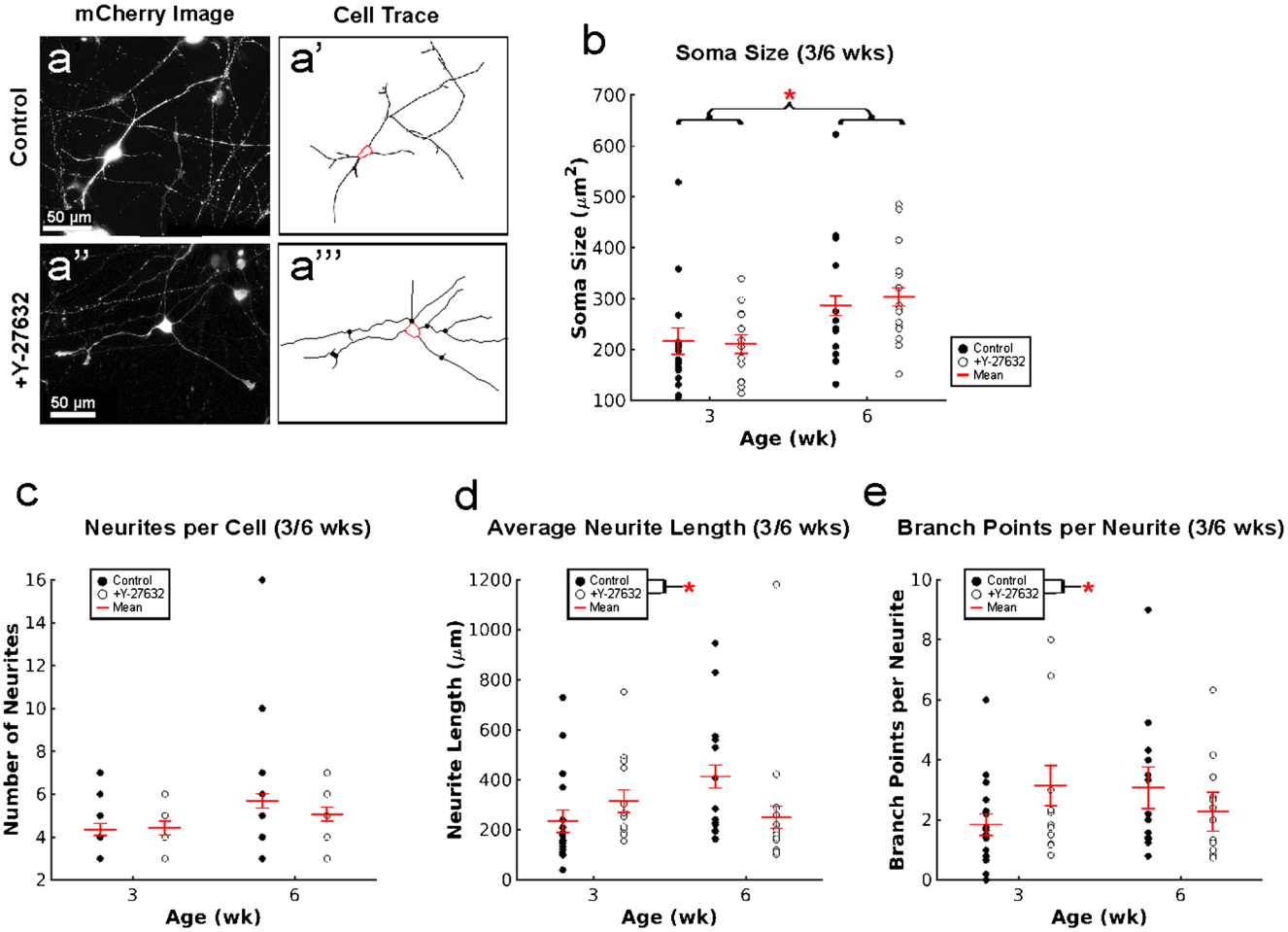

Fig. 2 Morphological effects of Y-27632 treatment at 3–6 weeks of age. **a** Representative images of neurons at 3 weeks of age stained for mCherry (**a**, **a**") and corresponding cell traces (**a'**, **a"'**) with (**a**", **a"'**) and without (**a**, **a'**) treatment with 10 μM Y-27632. **b** The average soma size of neurons increased significantly over time ($p = 0.0043$) but did not vary based on treatment ($p = 0.8303$). **c** There is no significant effect of age ($p = 0.0730$) or treatment ($p = 0.6132$) on the average number of neurites per cell. **d** There is no significant effect of age ($p = 0.3371$) or treatment ($p = 0.4833$) on the average neurite length but there is an interaction effect ($p = 0.0416$). **e** There is no significant effect of age ($p = 0.7137$) or treatment ($p = 0.6222$) on the average number of branch points per neurite but there is an interaction effect ($p = 0.0442$). All graphs: control $n = 17, 13$; Y-27632 $n = 14, 15$. Asterisk indicates $p < 0.05$. Double asterisks indicate $p < 0.001$ by 2-way ANOVA with post hoc HSD; data plotted as mean ± standard error of the mean; see Table 2 for complete statistics

the trough of each spike to the peak (see Fig. 2c); events greater than 10 mV in amplitude were considered action potentials. Action potentials that occurred within the 10 s + 25 pA pulse were counted as evoked activity, while those occurring at other times in 10-s trials were considered spontaneous.

Statistics

Unless otherwise indicated, *p* values are the result of a 1- or 2-way ANOVA for unbalanced design followed by *post hoc* Tukey HSD corrections for individual group comparisons and data are shown as mean ± standard error of the mean (SEM). For action potential amplitude, significance was assessed using a Wilcoxon signed-rank test. Statistics, data analysis and figure generation were performed using MATLAB (Natick, MA, USA) and CorelDRAW (Corel, Ottawa, Canada).

Results

Short-term ROCK inhibition increases neurite formation during the first 24 h of neuronal differentiation

To determine if ROCK inhibition increases initial neurite formation in iPSC-derived neuron cultures, neural progenitor cells (NPCs) were plated for terminal differentiation in neuron media containing 0, 5, 10, 25, or 50 μM Y-27632. After 24 h, cells were fixed and stained for DAPI and β-III-Tubulin (Fig. 1d). Automated morphological analysis

Table 1 Statistics for 24-h morphology experiments

Measurement-associated figure	Group	*N*	Mean	SEM	Statistics				
					One-way ANOVA *p* value	F (df)	Post hoc Tukey HSD *p* value		
							Group	vs Control	vs 5 μM
Number of neurites Fig. 1e	Control	42,747	0.75	0.0035	< 0.0001**	1762.92 (4)	Control		
	5 μM	51,526	1.00	0.0036			5 μM	< 0.0001**	
	10 μM	56,953	1.15	0.0037			10 μM	< 0.0001**	< 0.0001**
	25 μM	61,661	1.14	0.0038			25 μM	< 0.0001**	< 0.0001**
	50 μM	57,269	1.17	0.0038			50 μM	< 0.0001**	< 0.0001**
Average neurite length (μm) Fig. 1f	Control	22,002	38.64	0.2038	< 0.0001**	241.17 (4)	Control		
	5 μM	34,613	46.26	0.2446			5 μM	< 0.0001**	
	10 μM	41,918	50.19	0.2652			10 μM	< 0.0001**	< 0.0001**
	25 μM	44,864	49.74	0.2666			25 μM	< 0.0001**	< 0.0001**
	50 μM	42,537	51.50	0.2757			50 μM	< 0.0001**	< 0.0001**
Average branch points per neurite Fig. 1g	Control	22,002	0.5325	0.0054	< 0.0001**	144.13 (4)	Control		
	5 μM	34,613	0.6941	0.0065			5 μM	< 0.0001**	
	10 μM	41,918	0.7531	0.0067			10 μM	< 0.0001**	< 0.0001**
	25 μM	44,864	0.7658	0.0067			25 μM	< 0.0001**	< 0.0001**
	50 μM	42,537	0.7856	0.0068			50 μM	< 0.0001**	< 0.0001**

**$p<0.001$

using the CellInsight CX5 Screening Platform revealed that all of the treatments increased the number of neurites per cell ($p < 0.0001$, see Table 1 for full statistics), average neurite length ($p < 0.0001$) and average number of branch points per neurite ($p < 0.0001$) compared to control cells (Fig. 1c–f”’).

Rock inhibition by Y-27632 is expected to block neurite retraction, in part, through diminished myosin phosphorylation. Western blot analyses demonstrated that, relative to controls, NPCs treated for 24 h with 10 μM Y-27632 had significantly decreased levels of phosphorylated myosin regulatory light chain (pMLC) relative to tubulin (Fig. 1g–g’; control: pMLC::tubulin = 0.746 ± 0.0130, $n = 3$; Y-27632: 0.5651 ± 0.0104, $n = 3$, 3; t test $p < 0.0001$), thereby confirming that the inhibitor downregulates phosphorylation of known ROCK substrates in this cell line (Newell-Litwa et al. 2015).

Short-term ROCK inhibition does not cause a prolonged change in neurite morphology

To evaluate if early ROCK inhibition produced lasting morphological changes, neurons were cultured with or without 10 μM Y-27632 in the neuron media for the first 2 weeks of differentiation and then examined at two later time points. Cell morphology was examined by labeling cells with mCherry via viral transfection at 1 week of age. Cells were fixed at either 3 or 6 weeks of age and manually traced with Neurolucida software (Fig. 2a–a”’).

Soma size of iPSC-derived neurons increases with time in culture and correlates well with increased functional maturity (Bardy et al. 2016; Nicholas et al. 2013). Consistent with these findings, we observed that soma size was larger in 6-week-old cells compared to 3-week-old cells (Fig. 2b, $p = 0.0043$, 3 weeks 214.67 ± 16.42 μm^2, $n = 31$; 6 weeks 296.60 ± 21.70 μm^2, $n = 28$; see Table 2 for 3- and 6-week morphology statistics). Nonetheless, Y-27632 treatment did not affect soma size ($p = 0.8303$).

The average number of neurites per cell did not change based on drug treatment ($p = 0.6132$) or age group ($p = 0.0730$) (Fig. 2c). While neither drug treatment ($p = 0.4833$) nor age ($p = 0.3371$) alone caused a change in average neurite length, there was a significant interaction between the two factors based on multi-way ANOVA ($p = 0.0416$; control $n = 17$, 13; Y-27632 $n = 14$, 15) (Fig. 2d). A similar pattern was observed with the average number of branch points per neurite: neither treatment ($p = 0.6222$) nor age alone ($p = 0.7137$) affected the parameter but a significant interaction between the two was observed ($p = 0.0442$) (Fig. 2e).

The significant p value for the interaction of the two variables, condition and age, indicates that there may be a difference in how the values change with age based on the condition, even though none of the individual comparisons yielded a significant change. For example, while neither neurite length nor number of branch points per neurite showed any significant differences between individual age and drug treatment groups, in both cases, control cells showed a slight increase over time (neurite length 234.96 ± 45.10 μm to 413.93 ±

Table 2 Statistics for 3- and 6-week morphology experiments

Measurement-associated figure	Group	Age (weeks)	*N*	Mean	SEM	Statistics				
						Comparison	2-way ANOVA *p* value	F (df)	Post hoc Tukey HSD *p* value	
Soma size (μm^2) Fig. 2b	Control	3	17	217.36	26.27	Control vs Y-27632	0.8303	0.05 (1)		
		6	13	287.08	19.26					
		All	30	247.57	22.69					
	Y-27632	3	14	211.40	18.55	Age	0.0043*	8.85 (1)	3 vs 6	0.0043*
		6	15	304.85	17.93					
		All	29	259.74	17.74					
	All 3 weeks		31	214.67	16.42	Interaction	0.6669	0.19 (1)		
	All 6 weeks		28	296.60	21.70					
Number of neurites Fig. 2c	Control	3	17	4.35	0.27	Control vs Y-27632	0.6132	0.26 (1)		
		6	13	5.69	0.34					
		All	30	4.93	0.47					
	Y-27632	3	14	4.43	0.33	Age	0.0730	3.34 (1)		
		6	15	5.07	0.32					
		All	29	4.76	0.27					
	All 3 weeks		31	4.39	0.21	Interaction	0.5195	0.42 (1)		
	All 6 weeks		28	5.36	0.51					
Average neurite length (μm) Fig. 2d	Control	3	17	234.96	45.10	Control vs Y-27632	0.4833	0.50 (1)	C3 vs Y3	0.7495
		6	13	413.93	46.97				C6 vs Y6	0.2284
		All	30	312.51	42.67					
	Y-27632	3	14	315.85	45.26	Age	0.3371	0.94 (1)	C3 vs C6	0.1447
		6	15	250.35	43.72				Y3 vs Y6	0.8600
		All	29	281.97	42.12					
	All 3 weeks		31	271.49	32.40	Interaction	0.0416*	4.35 (1)	C3 vs Y6	0.9974
	All 6 weeks		28	326.30	51.66				R3 vs C6	0.6683
Average number of branch points per neurite Fig. 2e	Control	3	17	1.84	0.35	Control vs Y-27632	0.6222	0.25 (1)	C3 vs Y3	0.2604
		6	13	3.08	0.70				C6 vs Y6	0.7030
		All	30	2.38	0.35					
	Y-27632	3	14	3.14	0.67	Age	0.7137	0.14 (1)	C3 vs C6	0.3209
		6	15	2.28	0.65				Y3 vs Y6	0.6353
		All	29	2.70	0.38					
	All 3 weeks		31	2.43	0.37	Interaction	0.0442*	4.24 (1)	C3 vs Y6	0.9191
	All 6 weeks		28	2.65	0.36				Y3 vs C6	0.9998

*$p<0.05$

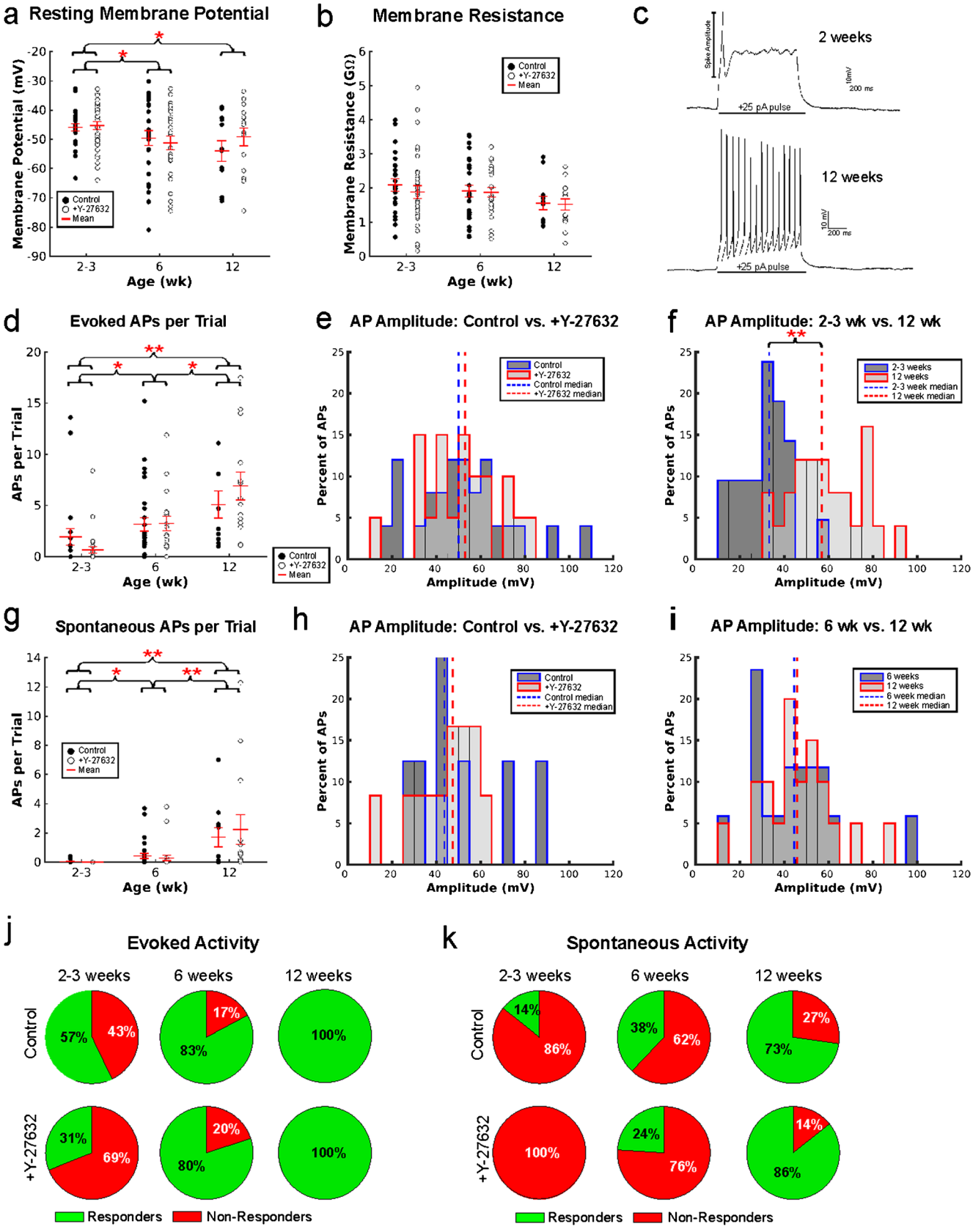
a Resting Membrane Potential
Membrane Potential (mV)
Age (wk)
Control
+Y-27632
Mean
b Membrane Resistance
Membrane Resistance (GΩ)
c
2 weeks
12 weeks
+25 pA pulse
d Evoked APs per Trial
APs per Trial
e AP Amplitude: Control vs. +Y-27632
Percent of APs
Amplitude (mV)
Control median
+Y-27632 median
f AP Amplitude: 2-3 wk vs. 12 wk
2-3 weeks
12 weeks
2-3 week median
12 week median
g Spontaneous APs per Trial
h AP Amplitude: Control vs. +Y-27632
i AP Amplitude: 6 wk vs. 12 wk
6 weeks
6 week median
j Evoked Activity
2-3 weeks
6 weeks
12 weeks
57%
43%
17%
83%
100%
31%
69%
20%
80%
100%
Responders
Non-Responders
k Spontaneous Activity
14%
86%
38%
62%
27%
73%
100%
24%
76%
14%
86%

◀ **Fig. 3** Electrophysiological effects of Y-27632 treatment at 2–3, 6 and 12 weeks of age. **a** The resting membrane potential (RMP) of neurons does not differ between treatment groups ($p = 0.4948$) but does become more hyperpolarized between 2 and 3 weeks of age and 6/12 weeks of age ($p = 0.0181$; post hoc HSD 3 vs 6 weeks $p = 0.0046$; 3 vs 12 weeks $p = 0.0426$; control $n = 25, 28, 12$; Y-27632 $n = 35, 27, 18$). **b** Membrane resistance does not change significantly by treatment group ($p = 0.5594$), or age ($p = 0.0938$; control $n = 25, 28, 12$; Y-27632: $n = 35, 27, 15$). **c** Representative traces at 2 weeks (top) and 12 weeks (bottom) of age in response to + 25 pA current pulse (bars). Amplitude of APs is measured from AP peak to trough (line, top). **d** Evoked APs per depolarizing pulse did not differ between treatment group ($p = 0.7548$) but does increase over time ($p < 0.0001$; post hoc HSD 2–3 vs 6 weeks $p = 0.0186$, 6 vs 12 weeks $p = 0.0032$, 2–3 vs 12 weeks $p < 0.0001$; control $n = 21, 29, 11$, Y-27632 $n = 29, 25, 13$). **e** Histogram of evoked AP amplitudes at 6 weeks of age shows no difference between treatments (Wilcoxon rank-sum $p = 0.9363$, control $p = 25$; Y-27632 $p = 20$). **f** Histogram comparing evoked AP amplitudes at 3 and 12 weeks of age shows a highly significant increase over time (Wilcoxon rank-sum test $p < 0.0001$; control $n = 12, 11$; Y-27632 $n = 8, 14$). **g** Spontaneous APs (APs occurring outside of the 1 s depolarizing current pulse) did not differ between treatment group ($p = 0.6897$) but does increase significantly between 2 and 3/6 and 12 weeks of age ($p < 0.0001$; post hoc HSD 6 vs 12 weeks $p < 0.0001$; 3 vs 12 weeks $p < 0.0001$; control $n = 21, 29, 11$; Y-27632 $n = 29, 25, 14$). **h** A histogram of spontaneous AP amplitudes at 12 weeks of age shows no difference between treatments (Wilcoxon rank-sum $p = 1$; control $n = 8$; Y-27632 $n = 12$). **i** A histogram comparing spontaneous AP amplitudes at 6 and 12 weeks of age shows no change over time (Wilcoxon rank-sum test $p = 0.6151$). **j** Percent of cells exhibiting evoked activity (responsive) vs cells that do not (non-responsive) for each treatment and time point. **k** Percent of cells exhibiting spontaneous activity (responsive) vs cells that do not (non-responsive) for each treatment and time point. Asterisk indicates $p < 0.05$; Double asterisks indicate $p < 0.001$ by 2-way ANOVA with post-hoc HSD; data in **a**, **b**, **d** and **g** are presented as mean ± standard error of the mean; see Table 3 for complete statistics

46.97 μm; number of branch points 1.84 ± 0.35 to 3.08 ± 0.70), while Y-27632-treated neurons showed a slight decrease over time (neurite length 315.85 ± 45.26 μm to 250.35 ± 43.72 μm; number of branch points 3.14 ± 2.51 to 2.28 ± 0.65). While neither trend was statistically significant, this result suggests that cultures may develop neurite length and complexity differently over time depending on whether ROCK inhibition had been applied early on in development.

Inhibition of ROCK does not affect electrophysiological properties of neurons

We next assessed electrophysiological properties of iPSC-derived neurons treated with 10 μM Y-27632 for the first week of differentiation. Electrophysiological measurements of iPSC-derived neurons were performed at three time points (2–3, 6 and 12 weeks). While Y-27632 had no effect on either resting membrane potential (Fig. 3a), or membrane resistance (Fig. 3b), the resting membrane potential of both treatment groups progressively hyperpolarized over time ($p = 0.0181$; control $n = 21, 29, 11$; Y-27632 $n = 29$ 25 14; see Table 3 for full electrophysiology statistics), increasing from − 45.51 mV ± 0.95 at the 2–3-week time point to − 51.34 mV ± 2.33 at 12 weeks. Membrane resistance tended to decrease with age ($p = 0.0938$; control $n = 21, 29, 11$; Y-27632 $n = 29, 25, 14$), with all groups averaging between 1 and 2 GΩ; however, this trend may partially result from the increased soma size observed over time (see Fig. 2b). The number of action potentials did not differ between control and Y-27632-treated neurons at any time point for either evoked or spontaneous activity ($p = 0.7548, 0.6897$; control $n = 21, 29, 11$; Y-27632 $n = 29, 25, 13$; Fig. 3d, g). However, the number of action potentials in both evoked ($p < 0.0001$) and spontaneous ($p < 0.0001$) activity increased significantly with age (Fig. 3d, g). The increase in average number of action potentials per trial is also reflected by an increase in the number of responsive cells (cells that fired at least once during the testing period) over time (Fig. 3j, k).

Finally, Y-27632 treatment did not alter the amplitude of either evoked or spontaneous action potentials (Fig. 3e, h). However, the amplitude of evoked action potentials increased with age (2–3 weeks 33.16 mV ± 12.10; 6 weeks 51.24 mV ± 23.28; 12 weeks 56.88 mV ± 25.84). The observed increase in action potential amplitude largely occurred between 3 and 6 weeks of age (Wilcoxon rank-sum, $p < 0.0001$). The amplitude of spontaneous action potentials did not change with age (Fig. 3i), possibly due to a lower sample size; very few cells produced spontaneous action potentials at 3 weeks of age (Fig. 3k).

Discussion

The ROCK inhibitor Y-27632 is routinely used in hiPSC culture, notably to improve cell survival after passaging. Given that it is well-tolerated and previous studies show that ROCK inhibition can promote neurite outgrowth (Newell-Litwa et al. 2015), we reasoned that Y-27632 treatment might accelerate the development of electrophysiological activity in hiPSC-derived neurons. As expected, we show that 24-h Y-27632 treatment increases neurite length, number and branching of iPSC-derived neurons (Fig. 1e–g', Table 1). This effect does not persist at 3 or 6 weeks of age (Fig. 2c–e, Table 2); however, we find that there is a trend towards an increase in neurite length and branching over time in control cells that is not present in the Y-27632-treated cells. This is not due to a difference in the overall neuron size, since the cell body area was unaffected by treatment (Fig. 2b). While the reason for this discrepancy is unclear, it is possible that short-term ROCK inhibition provides an early increase in morphological properties but this effect subsides after it is removed, while the control cells continue to develop. This interpretation is supported by the fact that at 3 weeks of age, the Y-27632-treated neurons exhibited a slightly increased number of neurites, neurite length and branch points per neurite compared to control neurons at 3 weeks of age. While not statistically robust, it is possible that a larger sample of cells would better test this

Table 3 Statistics for electrophysiology experiments

Measurement-associated figure	Group	Age (weeks)	*N*	Mean	SEM	Statistics				
						Comparison	2-way ANOVA *p* value	F (df)	Post hoc Tukey HSD *p* value	
Resting membrane potential Fig. 3a	Control	2–3	25	−45.90	1.2998	Control vs + Y-27632	0.4948	0.47 (1136)		
		6	28	−49.60	2.5933					
		12	12	−54.06	3.5366					
		All	65	−49.00	1.4130					
	Y-27632	2–3	35	−45.23	1.3516	Age groups	0.0181*	4.13 (2136)	2–3 vs 6	0.0446*
		6	27	−51.19	2.3238				6 vs 12	0.8801
		12	15	−49.17	3.0757				2–3 vs 12	0.0426*
		All	77	−48.09	1.2062	Interaction	0.4437	0.82 (2136)		
	All 2–3 weeks		60	−45.51	0.9499					
	All 6 weeks		55	−50.38	1.7320					
	All 12 weeks		27	−51.34	2.3257					
Membrane resistance Fig. 3b	Control	2–3	25	2.09	0.1839	Control vs + Y-27632	0.5594	0.34 (1136)		
		6	28	1.91	0.1739					
		12	12	1.56	0.1967					
		All	65	1.91	0.1102					
	Y-27632	2–3	35	1.88	0.1815	Age groups	0.0938	2.41 (2136)		
		6	27	1.88	0.1369					
		12	15	1.52	0.1634					
		All	77	1.81	0.1009	Interaction	0.8526	0.16 (2136)		
	All 2–3 weeks		60	1.97	0.1303					
	All 6 weeks		55	1.89	0.1102					
	All 12 weeks		27	0.54	0.1236					
Measurement-associated figure	Group	Age (weeks)	No. of cells	Mean	SEM	Statistics				
						Comparison	2-way ANOVA *p* value	F (df)	Post hoc Tukey HSD *p* value	
Evoked activity (number of action potentials per pulse) Fig. 3d	Control	2–3	21	1.92	0.8218	Control vs + Y-27632	0.7548	0.7548 (1123)		
		6	29	3.15	0.6637					
		12	11	5.09	1.3175					
		All	61	3.08	0.4972					
	Y-27632	2–3	29	0.65	0.3159	Age groups	< 0.0001 **	14.57 (2123)	2–3 weeks vs 6 weeks	0.0186*
		6	25	3.23	0.7002				6 weeks vs 12 weeks	0.0032*
		12	14	6.91	1.3718				2–3 weeks vs 12 weeks	< 0.0001**
		All	68	2.89	0.4898	Interaction	0.2082	1.59 (2123)		
	All 2–3 weeks		50	1.18	0.3962					
	All 6 weeks		54	3.19	0.7733					
	All 12 weeks		25	6.11	0.9608					

Table 3 (continued)

Measurement-associated figure	Group	Age (weeks)	No. of cells	Mean	SEM	Statistics				
						Comparison	2-way ANOVA *p* value	F (df)	Post hoc Tukey HSD *p* value	
Spontaneous activity (number of action potentials off-pulse) Fig. 3g	Control	2–3	21	0.04	0.0245	Control vs Y-27632	0.6897	0.16 (1123)		
		6	29	0.43	0.1754					
		12	11	1.71	0.6573					
		All	64	0.53	0.1597					
	Y-27632	2–3	29	0.00	0	Age groups	< 0.0001 **	14.39 (2123	2–3 weeks vs 6 weeks	0.4934
		6	25	0.29	0.1841				6 weeks vs 12 weeks	< 0.0001**
		12	14	2.24	1.0122				2–3 weeks vs 12 weeks	< 0.0001**
		All	68	0.57	0.2375	Interaction	0.6471	0.44 (2123)		
	All 2–3 weeks		50	0.02	0.0106					
	All 6 weeks		54	0.36	0.1262					
	All 12 weeks		25	2.00	0.6268					
Measurement-associated figure	Group	Age (weeks)	No. of cells	Median	Interquartile range	Statistics				
						Comparison	Wilcoxon rank-sum test			
Evoked activity (action potential amplitude) Fig. 3e/f	Control	2–3	12	32.93	9.13	Control vs + Y-27632	2–3 weeks	0.6441		
		6	25	50.09	24.97		6 weeks	0.9363		
		12	11	46.93	29.43		12 weeks	0.2180		
		All	48	44.29	24.93					
	Y-27632	2–3	9	33.80	15.31	Age groups	2–3 weeks vs 6 weeks	< 0.0001**		
		6	20	52.95	21.23		6 weeks vs 12 weeks	0.0955		
		12	14	61.93	16.83		2–3 weeks vs 12 weeks	< 0.0001**		
		All	29	41.60	25.09					
	All 2–3 weeks		21	33.16	12.10					
	All 6 weeks		45	51.42	23.28					
	All 12 weeks		25	56.88	25.84					
Spontaneous activity (action potential amplitude) Fig. 3h/i	Control	2–3	3	35.86	14.86	Control vs + Y-27632	2–3 weeks	N/A		
		6	11	51.90	19.88		6 weeks	0.0782		
		12	8	43.64	19.84		12 weeks	1.0000		
		All	22	43.52	21.59					
	Y-27632	2–3	0	0.00	0.00	Age groups	2–3 weeks vs 6 weeks	0.2040		
		6	6	31.12	14.07		6 weeks vs 12 weeks	0.6151		
		12	12	47.37	15.07		2–3 weeks vs 12 weeks	0.0913		
		All	18	45.13	24.99					
	All 2–3 weeks		3	35.86	19.82					
	All 6 weeks		17	44.37	25.41					
	All 12 weeks		20	45.61	20.05					

*$p<0.05$

**$p<0.001$

possibility. Additionally, treating cell cultures with Y-27632 for longer than 1 week may show results that more closely align with the morphological changes seen at 24 h.

Electrophysiological assays show no effect of Y-27632 treatment on either evoked or spontaneous firing properties (Fig. 3, Table 3). While ROCK inhibition did not affect the parameters we measured, we did observe increased electrophysiological maturity with age. While some neurons at every time point exhibited low levels of activity, we observed an increase in the total number of responsive neurons at later time points in both the control and Y-27632-treated cultures (Fig. 3j, k). Additionally, the number of action potentials observed in both evoked and spontaneous activity increased with age, as did the amplitude of evoked action potentials (Fig. 3d–g). The average resting membrane potential of cells also hyperpolarized over time (Fig. 3a).

In this study, we show patch clamp data from a total of 129 cells at three different ages. Numerous other studies reporting patch-clamp measurements from more than 100 neurons describe changes in functional maturity due to age or culture conditions (Bardy et al. 2015; Bardy et al. 2016; Belinsky et al. 2014; Bilican et al. 2014; Nicholas et al. 2013; Rushton et al. 2013). Despite significant differences in differentiation and electrophysiological protocols as well as the cell lines and ages tested, there are key commonalities that are observed in many of these reports that also align with our data. For example, reported values for resting membrane potential and membrane resistance are widely variable but there is consistently a more depolarized resting membrane potential and higher membrane resistance than is physiologically typical in mature neurons (Bardy et al. 2015; Belinsky et al. 2014; Bilican et al. 2014; Nicholas et al. 2013; Rushton et al. 2013). When reported, there is often a more hyperpolarized resting membrane potential and decreased membrane resistance in older cultures (Bilican et al. 2014; Nicholas et al. 2013; Rushton et al. 2013). Additionally, the majority of these studies demonstrate increased proportions of neurons exhibiting evoked or spontaneous activity in older cultures (Bardy et al. 2016; Bilican et al. 2014; Nicholas et al. 2013; Rushton et al. 2013). While Belinsky et al. reported only a weak developmental trend, the authors address that this is likely due to factors such as cell death in older cultures and the contribution of inactive neural precursors and neural progenitors at all ages. This latter phenomenon is also consistent with our data, as there are neurons in every age group that exhibit a low level of activity.

While there exists great heterogeneity among neuron types in the human brain, several electrophysiological features are generally consistent across subtypes. First, the resting membrane potential of mature cortical neurons is hyperpolarized and averages between − 60 and − 80 mV (Bean 2007; McCormick et al. 1985). This membrane potential is achieved by a highly regulated process of ion channel expression, particularly potassium channels and hyperpolarization occurs gradually over time as these channels are expressed (Swayne and Wicki-Stordeur 2012). This observation is correlated with an age-dependent decrease in membrane resistance. These electrophysiological changes are observed in both rodents and in human tissue (Moore et al. 2009; Picken Bahrey and Moody 2003; Spitzer 2006; Swayne and Wicki-Stordeur 2012). The development of electrical activity is also a hallmark for the maturation of neuronal function and is key in many other aspects of early neurodevelopment (Spitzer 2006). This process is largely controlled by the development of voltage-gated ion channels (Picken Bahrey and Moody 2003; Song et al. 2013).

Overall, our study suggests that iPSC-derived neurons possess electrophysiological properties that are consistent with 2nd trimester fetal tissue, when compared with the properties of human fetal cerebral cortex (Moore et al. 2009; Moore et al. 2011). Given the relatively brief culture durations, as compared with the development of the human nervous system, the conclusion that iPSC-derived neurons are electrophysiologically immature is not necessarily surprising. Herein, we attempted to accelerate maturation by manipulating processes known to regulate morphological maturation. Many alternative strategies have been employed towards a similar end, including astrocyte co-culture (Johnson et al. 2007; Kuijlaars et al. 2016; Tang et al. 2013), 3D culturing (Lancaster et al. 2013; Pasca et al. 2015; Yan et al. 2016) and specialized culture media that is formulated to promote neuron activity or mimic the early-stage in vivo environment more closely (Bardy et al. 2015; Kemp et al. 2016).

While we did not succeed in accelerating the timeline of electrophysiological or long-term morphological maturity, we reaffirmed the efficacy of inhibiting ROCK activity as a means of enhancing initial neurite formation and it is possible that including a ROCK inhibitor long-term during cell culture would result in a sustained effect on morphological and perhaps electrophysiological, properties. This study also reaffirms many functional phenotypes that are shared in the existing literature, including underlining the importance of culture duration in neuronal properties. Moving forward, it will be critical to consider these factors when using iPSC-derived neurons as a model system.

Acknowledgments We wish to thank Kristen Brennand (Icahn School of Medicine at Mount Sinai) for providing the neurotypic iPSC line used in this study. We also thank Keena Thomas and Amy Bouton for assistance with the pMLC Western blot. Additionally, we would like to thank Peter Klein and Adam Lu for help with figure generation and statistics, Ruth Stornetta for help in the neurite tracing experiments and Neurolucida software and Stefan Bekiranov for valuable conversations on statistics.

Funding information LJH and NM received support from a neuroscience training grant (NIH/NIGM T32GM008328-24). MPB is supported by NIH Grant R01NS099586-01. MJM is supported by NIMH U01 MH106882 and the Owens Philanthropic Fund. KJL was supported by a Hartwell Post-doctoral Fellowship.

References

Amano M, Fukata Y, Kaibuchi K (2000) Regulation and functions of Rho-associated kinase. Exp Cell Res 261:44–51. https://doi.org/10.1006/excr.2000.5046

Bardy C et al (2015) Neuronal medium that supports basic synaptic functions and activity of human neurons in vitro. Proc Natl Acad Sci U S A 112:E2725–E2734. https://doi.org/10.1073/pnas.1504393112

Bardy C et al (2016) Predicting the functional states of human iPSC-derived neurons with single-cell RNA-seq and electrophysiology. Mol Psychiatry 21:1573–1588. https://doi.org/10.1038/mp.2016.158

Bean BP (2007) The action potential in mammalian central neurons. Nat Rev Neurosci 8:451–465. https://doi.org/10.1038/nrn2148

Belinsky GS, Rich MT, Sirois CL, Short SM, Pedrosa E, Lachman HM, Antic SD (2014) Patch-clamp recordings and calcium imaging followed by single-cell PCR reveal the developmental profile of 13 genes in iPSC-derived human neurons. Stem Cell Res 12:101–118. https://doi.org/10.1016/j.scr.2013.09.014

Bellin M, Marchetto MC, Gage FH, Mummery CL (2012) Induced pluripotent stem cells: the new patient? Nat Rev Mol Cell Biol 13:713–726. https://doi.org/10.1038/nrm3448

Bilican B et al (2014) Physiological normoxia and absence of EGF is required for the long-term propagation of anterior neural precursors from human pluripotent cells. PLoS One 9:e85932. https://doi.org/10.1371/journal.pone.0085932

Bradford AB, McNutt PM (2015) Importance of being Nernst: synaptic activity and functional relevance in stem cell-derived neurons. World J Stem Cells 7:899–921. https://doi.org/10.4252/wjsc.v7.i6.899

Brennand KJ et al (2015) Creating patient-specific neural cells for the in vitro study of brain disorders. Stem Cell Reports 5:933–945. https://doi.org/10.1016/j.stemcr.2015.10.011

Brennand KJ, Simone A, Jou J, Gelboin-Burkhart C, Tran N, Sangar S, Li Y, Mu Y, Chen G, Yu D, McCarthy S, Sebat J, Gage FH (2011) Modelling schizophrenia using human induced pluripotent stem cells. Nature 473(7346):221–225

Chan CC, Khodarahmi K, Liu J, Sutherland D, Oschipok LW, Steeves JD, Tetzlaff W (2005) Dose-dependent beneficial and detrimental effects of ROCK inhibitor Y27632 on axonal sprouting and functional recovery after rat spinal cord injury. Exp Neurol 196:352–364. https://doi.org/10.1016/j.expneurol.2005.08.011

Chinchalongporn V, Koppensteiner P, Pre D, Thangnipon W, Bilo L, Arancio O (2015) Connectivity and circuitry in a dish versus in a brain. Alzheimers Res Ther 7:44. https://doi.org/10.1186/s13195-015-0129-y

Fournier AE, Takizawa BT, Strittmatter SM (2003) Rho kinase inhibition enhances axonal regeneration in the injured. J Neurosci 23:1416–1423

Gu H, Yu SP, Gutekunst CA, Gross RE, Wei L (2013) Inhibition of the Rho signaling pathway improves neurite outgrowth and neuronal differentiation of mouse neural stem cells. Int J Physiol Pathophysiol Pharmacol 5:11–20

Hall A (1998) Rho GTPases and the actin cytoskeleton. Science 279:509–514

Jia XF, Ye F, Wang YB, Feng DX (2016) ROCK inhibition enhances neurite outgrowth in neural stem cells by upregulating YAP expression in vitro. Neural Regen Res 11:983–987. https://doi.org/10.4103/1673-5374.184499

Johnson MA, Weick JP, Pearce RA, Zhang SC (2007) Functional neural development from human embryonic stem cells: accelerated synaptic activity via astrocyte coculture. J Neurosci 27:3069–3077. https://doi.org/10.1523/JNEUROSCI.4562-06.2007

Kemp PJ et al (2016) Improving and accelerating the differentiation and functional maturation of human stem cell-derived neurons: role of extracellular calcium and GABA. J Physiol 594:6583–6594. https://doi.org/10.1113/JP270655

Kubo T, Hata K, Yamaguchi A, Yamashita T (2007) Rho-ROCK inhibitors as emerging strategies to promote nerve regeneration. Curr Pharm Des 13:2493–2499

Kuijlaars J et al (2016) Sustained synchronized neuronal network activity in a human astrocyte co-culture system. Sci Rep 6:36529. https://doi.org/10.1038/srep36529

Kurosawa H (2012) Application of Rho-associated protein kinase (ROCK) inhibitor to human pluripotent stem cells. J Biosci Bioeng 114:577–581. https://doi.org/10.1016/j.jbiosc.2012.07.013

Lam RS, Topfer FM, Wood PG, Busskamp V, Bamberg E (2017) Functional maturation of human stem cell-derived neurons in long-term cultures. PLoS One 12:e0169506. https://doi.org/10.1371/journal.pone.0169506

Lancaster MA et al (2013) Cerebral organoids model human brain development and microcephaly. Nature 501:373–379. https://doi.org/10.1038/nature12517

Lingor P, Teusch N, Schwarz K, Mueller R, Mack H, Bahr M, Mueller BK (2007) Inhibition of Rho kinase (ROCK) increases neurite outgrowth on chondroitin sulphate proteoglycan in vitro and axonal regeneration in the adult optic nerve in vivo. J Neurochem 103:181–189. https://doi.org/10.1111/j.1471-4159.2007.04756.x

Livesey MR, Magnani D, Hardingham GE, Chandran S, Wyllie DJ (2016) Functional properties of in vitro excitatory cortical neurons derived from human pluripotent stem cells. J Physiol 594:6573–6582. https://doi.org/10.1113/JP270660

Luo L (2000) Rho GTPases in neuronal morphogenesis. Nat Rev Neurosci 1:173–180. https://doi.org/10.1038/35044547

Machesky LM, Hall A (1997) Role of actin polymerization and adhesion to extracellular matrix in Rac- and Rho-induced cytoskeletal reorganization. J Cell Biol 138:913–926

McCormick DA, Connors BW, Lighthall JW, Prince DA (1985) Comparative electrophysiology of pyramidal and sparsely spiny stellate neurons of the neocortex. J Neurophysiol 54:782–806. https://doi.org/10.1152/jn.1985.54.4.782

Minase T, Ishima T, Itoh K, Hashimoto K (2010) Potentiation of nerve growth factor-induced neurite outgrowth by the ROCK inhibitor Y-27632: a possible role of IP(3) receptors. Eur J Pharmacol 648:67–73. https://doi.org/10.1016/j.ejphar.2010.09.007

Moe MC et al (2005) Multipotent progenitor cells from the adult human brain: neurophysiological differentiation to mature neurons. Brain 128:2189–2199. https://doi.org/10.1093/brain/awh574

Moore AR, Filipovic R, Mo Z, Rasband MN, Zecevic N, Antic SD (2009) Electrical excitability of early neurons in the human cerebral cortex during the second trimester of gestation. Cereb Cortex 19:1795–1805. https://doi.org/10.1093/cercor/bhn206

Moore AR, Zhou WL, Jakovcevski I, Zecevic N, Antic SD (2011) Spontaneous electrical activity in the human fetal cortex in vitro. J Neurosci 31:2391–2398. https://doi.org/10.1523/JNEUROSCI.3886-10.2011

Newell-Litwa KA, Badoual M, Asmussen H, Patel H, Whitmore L, Horwitz AR (2015) ROCK1 and 2 differentially regulate actomyosin organization to drive cell and synaptic polarity. J Cell Biol 210:225–242. https://doi.org/10.1083/jcb.201504046

Nicholas CR et al (2013) Functional maturation of hPSC-derived forebrain interneurons requires an extended timeline and mimics human neural development. Cell Stem Cell 12:573–586. https://doi.org/10.1016/j.stem.2013.04.005

Pasca AM et al (2015) Functional cortical neurons and astrocytes from human pluripotent stem cells in 3D culture. Nat Methods 12:671–678. https://doi.org/10.1038/nmeth.3415

Picken Bahrey HL, Moody WJ (2003) Early development of voltage-gated ion currents and firing properties in neurons of the mouse cerebral cortex. J Neurophysiol 89:1761–1773. https://doi.org/10.1152/jn.00972.2002

Pre D et al (2014) A time course analysis of the electrophysiological properties of neurons differentiated from human induced pluripotent stem cells (iPSCs). PLoS One 9:e103418. https://doi.org/10.1371/journal.pone.0103418

Randall AD (2016) Are stem cell-derived neural cells physiologically credible? J Physiol 594:6569–6572. https://doi.org/10.1113/JP273348

Roloff F, Scheiblich H, Dewitz C, Dempewolf S, Stern M, Bicker G (2015) Enhanced neurite outgrowth of human model (NT2) neurons by small-molecule inhibitors of Rho/ROCK signaling. PLoS One 10:e0118536. https://doi.org/10.1371/journal.pone.0118536

Rushton DJ, Mattis VB, Svendsen CN, Allen ND, Kemp PJ (2013) Stimulation of GABA-induced Ca2+ influx enhances maturation of human induced pluripotent stem cell-derived neurons. PLoS One 8:e81031. https://doi.org/10.1371/journal.pone.0081031

Song M, Mohamad O, Chen D, Yu SP (2013) Coordinated development of voltage-gated Na+ and K+ currents regulates functional maturation of forebrain neurons derived from human induced pluripotent stem cells. Stem Cells Dev 22:1551–1563. https://doi.org/10.1089/scd.2012.0556

Spitzer NC (2006) Electrical activity in early neuronal development. Nature 444:707–712. https://doi.org/10.1038/nature05300

Swayne LA, Wicki-Stordeur L (2012) Ion channels in postnatal neurogenesis: potential targets for brain repair. Channels (Austin) 6:69–74. https://doi.org/10.4161/chan.19721

Takahashi K, Tanabe K, Ohnuki M, Narita M, Ichisaka T, Tomoda K, Yamanaka S (2007) Induction of pluripotent stem cells from adult human fibroblasts by defined factors. Cell 131:861–872. https://doi.org/10.1016/j.cell.2007.11.019

Tan HB, Zhong YS, Cheng Y, Shen X (2011) Rho/ROCK pathway and neural regeneration: a potential therapeutic target for central nervous system and optic nerve damage. Int J Ophthalmol 4:652–657. https://doi.org/10.3980/j.issn.2222-3959.2011.06.16

Tang X, Zhou L, Wagner AM, Marchetto MC, Muotri AR, Gage FH, Chen G (2013) Astroglial cells regulate the developmental timeline of human neurons differentiated from induced pluripotent stem cells. Stem Cell Res 11:743–757. https://doi.org/10.1016/j.scr.2013.05.002

Watanabe K et al (2007) A ROCK inhibitor permits survival of dissociated human embryonic stem cells. Nat Biotechnol 25:681–686. https://doi.org/10.1038/nbt1310

Weick JP (2016) Functional properties of human stem cell-derived neurons in health and disease. Stem Cells Int 2016:4190438. https://doi.org/10.1155/2016/4190438

Yan Y, Song L, Tsai AC, Ma T, Li Y (2016) Generation of neural progenitor spheres from human pluripotent stem cells in a suspension bioreactor. Methods Mol Biol 1502:119–128. https://doi.org/10.1007/7651_2015_310

Yang P, Wen HZ, Zhang JH (2010) Expression of a dominant-negative Rho-kinase promotes neurite outgrowth in a microenvironment mimicking injured central nervous system. Acta Pharmacol Sin 31:531–539. https://doi.org/10.1038/aps.2010.35